Differential Geometry and its Applications 49 (2016) 43–64

Contents lists available at ScienceDirect

Differential Geometry and its Applications

www.elsevier.com/locate/difgeo

Riemannian and Finslerian spheres with fractal cut loci

Jin-ichi Itoh [a,1], Sorin V. Sabau [b,*,2]

[a] *Faculty of Education, Kumamoto University, Kumamoto 860, Japan*
[b] *School of Science, Dep. of Mathematics, Tokai University, Sapporo 005-8600, Japan*

A R T I C L E   I N F O

Article history:
Received 23 December 2014
Received in revised form 2 May 2016
Available online xxxx
Communicated by Z. Shen

MSC:
58B20
53C22

Keywords:
Riemannian manifolds
Non-reversible Finsler manifolds
Geodesics
Cut locus
Hausdorff measure
Fractals

A B S T R A C T

The present paper shows that for a given integer $k \geq 2$ it is possible to construct an at least k-differentiable Riemannian metric on the sphere of a certain dimension such that the cut locus of a point of it becomes a fractal. Moreover, we show that this construction can be extended to the case of Finslerian spheres as well.

1. Introduction

The cut locus $\mathcal{C}(p)$ of a point p in a Riemannian or Finsler manifold is, roughly speaking, the set of all other points for which there are multiple minimizing geodesics connecting them from p. Of course, in some special cases, it may contain additional points where the minimizing geodesic is unique.

The notion of cut locus was introduced and studied for the first time by H. Poincaré in 1905 for the Riemannian case. Later on, in the case of a two dimensional analytical sphere, S. B. Myers has proved in 1935 that the cut locus of a point is a finite tree [10] in both Riemannian and Finslerian cases. Moreover, in the case of an analytic Riemannian manifold, M. Buchner has shown the triangulability of $\mathcal{C}(p)$ [2], and has determined its local structure for the low dimensional case [3] in 1977 and 1978, respectively.

Despite the vast literature existing for the Riemannian case, the investigations of the cut locus of a Finsler manifolds are scarce (see [1,7,9,12,13]).

* Corresponding author.
E-mail addresses: j-itoh@kumamoto-u.ac.jp (J. Itoh), sorin@tokai.ac.jp (S.V. Sabau).

[1] The first author was partially supported by Grant-in Aid for Scientific Research (C) 26400072.
[2] The second author was partially supported by Grant-in Aid for Scientific Research (C) 22540097.

http://dx.doi.org/10.1016/j.difgeo.2016.07.004

Recently, it was shown that the cut locus of a closed subset N of a Finsler surface has the structure of a local tree being a union of rectifiable Jordan arcs [14]. Even though the results are similar to the Riemannian case, showing that there is nothing special about the metric structure to be Riemannian, one should always pay attention to the fact that, unlike its Riemannian correspondent, the Finslerian distance is not symmetric, so the proofs and arguments are quite different.

Returning to the Riemannian case, in the case of an arbitrary metric, the cut locus of a point can have a very complicated structure. For example, H. Gluck and D. Singer have constructed a C^∞ Riemannian manifold that has a point whose cut locus is not triangulable [5].

There is a closed relationship between the complexity of the cut locus and the regularity of the metric, regardless if it is Riemannian or Finslerian. Indeed, if the metric has a certain degree of regularity, then the cut locus of a point may enjoy a simple structure. However, if the metric loses its regularity, the cut locus might become a very complicated set, for example a fractal. Recall that, roughly speaking, a fractal is a set whose Hausdorff dimension is not an integer (see [4] for alternative definitions and examples), the fact that makes fractals typical examples of what we call "complicated sets".

Let us mention that the cut locus of any point on a C^∞ Riemannian manifold cannot be a fractal (see [8]). However, there is a $C^{1,1}$ Riemannian metric on the two dimensional sphere $\mathbb{S}^2$ and a point $p \in \mathbb{S}^2$ such that the total length of $\mathcal{C}(p)$ is infinite (see [6]).

Motivated by all these, in the present paper, we are going to study the following two questions:

1. *Does there exist Riemannian metrics having points whose cut locus is a fractal?*
2. *Are there more general metric structures, for example Finsler metrics, with the same property?*

The answer to both questions above is affirmative. Indeed, in the present paper we construct an at least k differentiable, $2 \leq k < \infty$, Riemannian metric on a topological sphere $\mathbb{S}^n$, provided the dimension n is high enough, namely, we prove

Theorem 1.1. *For any integer $2 \leq k < \infty$ there is an at least k-differentiable Riemannian metric on the $n(k)$-dimensional sphere $\mathbb{S}^{n(k)}$ and a point p in $\mathbb{S}^{n(k)}$ such that the Hausdorff dimension of $\mathcal{C}(p)$ is a real number between 1 and 2, where $n(k) := \frac{3^{k-1}+3}{2}$.*

Moreover, we show that there is a Finsler metric of Randers type on this sphere with the same property. Indeed, if we use the same notations as in Theorem 1.1, we have

Theorem 1.2. *For any integer $2 \leq k < \infty$, under the influence of a suitable magnetic field β defined on $\mathbb{S}^{n(k)}$, there is an at least k-differentiable non-Riemannian Finsler metric of Randers type on $\mathbb{S}^{n(k)}$ such that the cut locus of the point p with respect to this Finsler metric coincides with $\mathcal{C}(p)$.*

Acknowledgements We express our gratitude to H. Shimada for many useful discussions during the preparation of this manuscript.

2. Basic construction

In this section, we will construct:

- an infinite tree IT in $\mathbb{R}^n$ with the end points set E,
- a closed, convex ball H in $\mathbb{R}^n$ with C^1-boundary that contains IT and $E \subset \partial H$.

The set E is actually a fractal whose Hausdorff dimension is a value between 1 and 2 (see [4] for definitions).

We begin by defining three infinite series of numbers

$$
\begin{aligned}
t_i &:= \left(\frac{1}{3^{k-1}}\right)^i, \qquad i \in \{0,1,\dots\}\\
l_i &:= \frac{t_i}{\sin(\frac{\phi}{3^i})}, \qquad i \in \{0,1,\dots\}\\
r_i &:= \sum_{\nu=i+1}^{\infty} l_\nu \cos(\frac{\phi}{3^\nu}), \qquad i \in \{-1,0,1,\dots\},
\end{aligned}
\tag{2.1}
$$

where $\phi \in (0, \frac{\pi}{2})$ is an arbitrary fixed angle and $k \geq 2$ a fixed integer.

One can easily see that (t_i), (l_i) and (r_i) are monotone decreasing series that converge to zero, for $i \to \infty$.

We will use these in order to construct a fractal set in $\mathbb{R}^n$. For the moment we do not assume any relation between n and k.

Let us consider in $\mathbb{R}^n$ the points o, q, q_0, $\dots$, $q_{j_1 j_2 \dots j_m}$, where $m \in \{1,2,\dots\}$, $i \in \{1,2,\dots,m\}$, and $j_i \in \{-(n-1),\dots,-1,0,1,\dots,n-1\}$ are defined as follows.

$$
o := (0,0,\dots,0), \qquad q := (l_0, 0, \dots, 0), \tag{2.2}
$$

$\boxed{m = 1}$

$$
\begin{aligned}
q_0 &:= (l_0 + l_1, 0, \dots, 0)\\
q_{j_1} &:= (l_0 + l_1 \cos(\frac{\phi}{3}), 0, \dots, 0, \underset{|j_1|+1}{\widehat{l_1 \sin(\frac{\phi}{3}) a_1}}, 0, \dots, 0),
\end{aligned}
\tag{2.3}
$$

where $j_1 \in \{-(n-1),\dots,-1,0,1,\dots,n-1\}$, the symbol $\hat{}$ shows the position of a component in a vector, and $|\cdot|$ is the usual absolute value of a real number;

$\boxed{m > 1}$

$$
\begin{aligned}
q_{\underbrace{0\dots0}_{m}} &:= (\sum_{i=0}^{m} l_i, 0, \dots, 0)\\
q_{\underbrace{0\dots j_m}_{m}} &:= (\sum_{i=0}^{m-1} l_i + l_m \cos(\frac{\phi}{3^m}), 0, \dots, 0, \underset{|j_m|+1}{\widehat{l_1 \sin(\frac{\phi}{3^m}) a_m}}, 0, \dots, 0),\\
q_{j_1 j_2 \dots j_m} &:= R^{|j_1|+1}(q, \frac{\phi}{3} a_1) \circ R^{|j_2|+1}(q, \frac{\phi}{3^2} a_2) \circ \dots\\
&\quad \circ R^{|j_{m-1}|+1}(q_{j_1 j_2 \dots j_{m-1}} \frac{\phi}{3^{m-1}} a_{m-1}) \circ q_{00\dots j_m},
\end{aligned}
\tag{2.4}
$$

where

$$
a_i := \begin{cases} -1, & \text{if } j_i < 0\\ 0, & \text{if } j_i = 0\\ 1, & \text{if } j_i > 0 \end{cases}, \tag{2.5}
$$

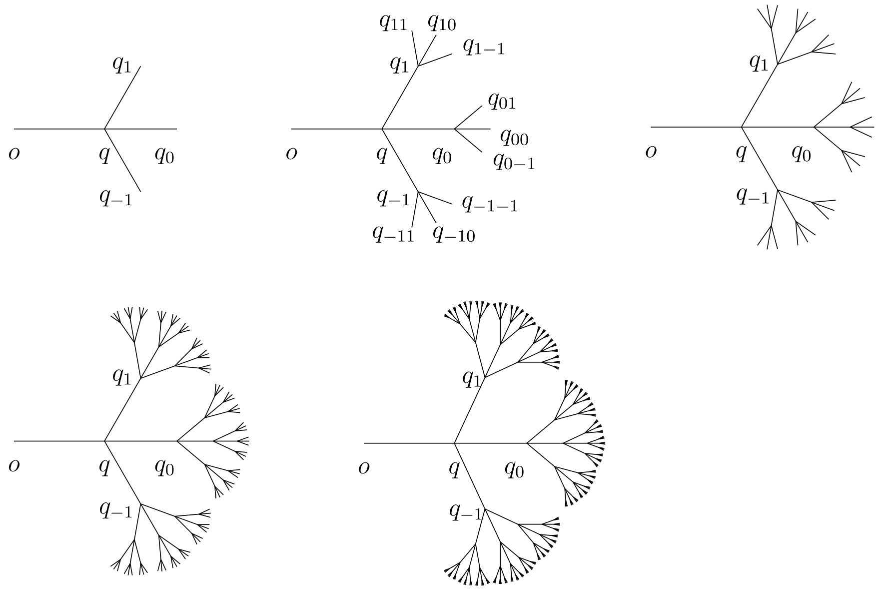

Fig. 1. The tree IT_m in $\mathbb{R}^2$ for $m = 1, 2, 3, 4, 5$, respectively.

and $R^j(x, \theta)$ is the rotation of angle θ around the affine subspace that is orthogonal to the $< e_1, e_j >$ plane and contains x. Here e_j is the unit vector with all components zero except the j-th component which is 1, namely

$$e_j = (0, \dots, \underset{\hat{j}}{1}, \dots, 0),$$

$x \in \{q_{j_1 j_2 \dots j_m} : j_1, j_2, \dots j_m \text{ as above}\}$ and $\theta \in \{\frac{\phi}{3^i} : i = 1, \dots, m-1\}$.

One can easily see that the points $q_{j_1 j_2 \cdots j_{m-1} *}$ are all on the sphere with center $q_{j_1 j_2 \cdots j_{m-1}}$ and radius l_m, for any fixed $m > 0$ and j_i, $i \in \{1, 2, \dots, m\}$.

For later use we denote the segment between o and q by s, the segment between q and q_{j_1} by s_{j_1} and so on inductively, such that the segment between $q_{j_1 j_2 \cdots j_{m-1}}$ and $q_{j_1 j_2 \cdots j_m}$ will be denoted by $s_{j_1 j_2 \cdots j_{m-1} j_m}$.

Likely, we denote the ray from o that contains q by γ, the ray from q that contains s_{j_1} by γ_{j_1} and so on inductively, such that the ray from $q_{j_1 j_2 \cdots j_{m-1}}$ that contains $s_{j_1 j_2 \cdots j_{m-1} j_m}$ will be denoted by $\gamma_{j_1 j_2 \cdots j_{m-1} j_m}$.

Let $IT_0 := \{s\}$, $IT_m := \cup_{i=1}^m \{s_{j_1 j_2 \cdots j_{m-1} j_m}\}$ be the union of segments $s_{j_1 j_2 \cdots j_{m-1} j_m}$, $IT := \lim_{m \to \infty} IT_m$ be the infinite tree and let $Q := \cup_{m=1}^{\infty} \{q_{j_1 j_2 \cdots j_{m-1} j_m}\}$ be the set of points $q_{j_1 j_2 \cdots j_{m-1} j_m}$.

Taking into account (2.1) and the construction above, one can see that $\lim_{i \to \infty} l_1 = 0$ implies $L := \sum_{i=0}^{\infty} l_i$ is finite, therefore the edges cannot prolong to infinity, so the set Q must have a subset of limit points $E \subset Q$.

The set E is in fact the set of *end points* of the infinite tree IT, except the root point o (see Fig. 1). Moreover, one can see that IT is completely contained in the ball with center o and radius L.

Remark 2.1. Remark that for the infinite tree IT in $\mathbb{R}^n$, there are $2n - 1$ branches that ramify from each node. The maximum depth level in the tree is given by m and the branches and nodes at a given depth level i are specified by j_i. Fig. 1 shows the growth of the tree IT in the case $\mathbb{R}^2$, namely a tree with three branches that ramify from each node at each level.

Next, we will construct a closed, convex ball H in $\mathbb{R}^n$ with C^1-boundary as follows:

- take a point $\hat{q}$ on the straight line γ such that $d(0, \hat{q}) = \frac{r_{-1}}{\cos \phi}$, where d is the usual Euclidean distance;

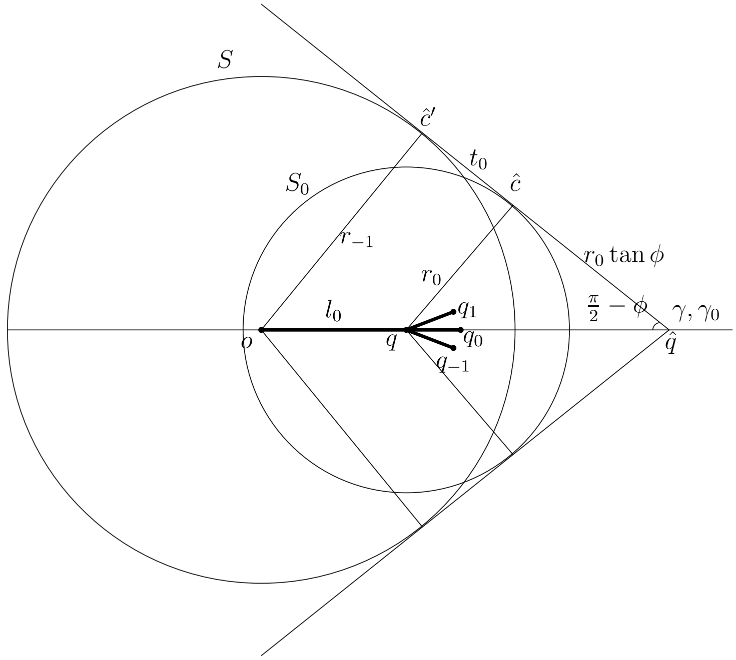

Fig. 2. A longitudinal section in the cone C in the case $IT_1 \subset \mathbb{R}^3$.

- consider the right circular cone C with vertex $\hat{q}$, axis γ and vertex angle $\pi - 2\phi$;
- consider the $(n-1)$-spheres $S_0 = S(q, r_0)$ and $S = S(o, r_{-1})$ in $\mathbb{R}^n$ of center q and o, and radii r_0 and r_{-1}, respectively.

Then, it can be verified by simple trigonometric computations that the right circular cone C is exterior tangent to the spheres S_0 and S (see Fig. 2). The intersection of C with the spheres S_0 and S is made of the $(n-2)$-spheres c and c', respectively (in the case $IT \subset \mathbb{R}^3$ these are circles).

Remark that the $(n-2)$-spheres c and c' cut out:

- a truncated cone $A \subset C$, from the cone C;
- a small spherical cap P_0 with boundary $c \cap S_0$ from the sphere S_0;
- a large spherical cap P with boundary $c' \cap S$ from the sphere S.

Gluing at the both ends of the truncated cone A_0 the spherical caps mentioned above we obtain a closed, convex ball $H_0 \subset \mathbb{R}^n$ whose boundary is a C^1-hypersurface $\partial H_0 \subset \mathbb{R}^n$ (see Fig. 3).

We remark that the (inward) cut locus of H_0 endowed with the induced Euclidean norm from $\mathbb{R}^n$ is exactly the segment s. Indeed, the inward geodesic rays from ∂H_0 concentrates at a point $\hat{u} \in s$. The same length inward geodesic rays orthogonal to the cloth of the truncated cone A_0, emanating from an arbitrary point of the $(n-2)$-sphere

$$c_u := \{x \in A | d(x, \hat{q}) = (d(o, \hat{q}) - u)\sin\phi\},$$

concentrate at a point $\hat{u} := (u, 0, \dots, 0) \in s \setminus \{o, q\}$, the inward geodesic rays of same length from the small spherical cap of S_0 concentrate at q and similarly the geodesic rays from the large spherical cap of S concentrate at o.

Therefore, given a segment $s = oq \subset IT$ we obtain a C^1-hypersurface $\partial H_0 \in \mathbb{R}^n$ whose (inward) cut locus and conjugate locus is exactly the segment s.

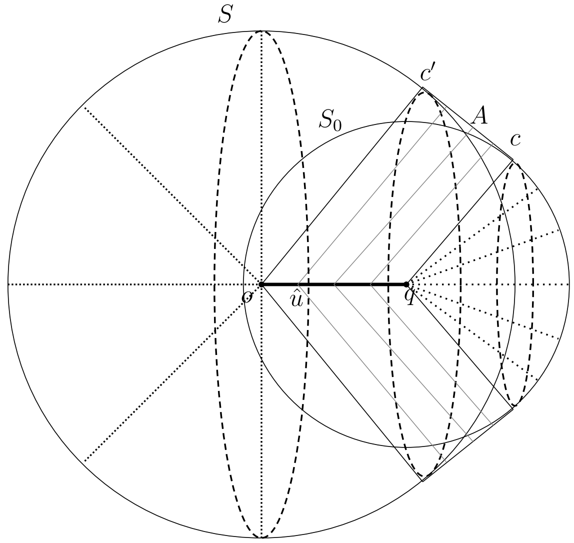

Fig. 3. The segment $s = oq$ is the inward cut locus of the C^1-hypersurface ∂H_0 in the case $IT_0 \subset \mathbb{R}^3$.

Let us see how this construction looks like at next step. Consider $m = 1$ and therefore our tree becomes $IT_1 = \{s, s_{j_1} | j_1 \in \{-(n-1), \dots, 0, 1, \dots, n-1\}\}$. The construction reads now:

- take a set of points $\hat{q}_{j_1}$ on the straight line γ_{j_1} such that $d(q, \hat{q}_{j_1}) = \frac{r_0}{\cos \frac{\phi}{3}}$;
- consider the right circular cones C_{j_1} with vertices $\hat{q}_{j_1}$, axes γ_{j_1} and vertex angles $\pi - 2\frac{\phi}{3}$;
- consider the $(n-1)$-spheres $S_{j_1} = S(q_{j_1}, r_1)$ and $S_0 = S(q, r_0)$ in $\mathbb{R}^n$.

The right circular cones C_{j_1} are exterior tangent to the spheres S_{j_1} and S_0. The intersection of C_{j_1} with the spheres S_{j_1} and S_0 is made of $2n-1$ spheres $c_{j_1} := C_{j_1} \cap S_{j_1}$ and $c^0_{j_1} =: C_{j_1} \cap S_0$, respectively, that cut off

- $2n-1$ truncated cones $A_{j_1} \subset C_{j_1}$, from the cone C_{j_1};
- $2n-1$ small spherical caps, from the spheres S_{j_1}, whose boundaries are $C_{j_1} \cap S_{j_1}$;
- $2n-1$ large spherical caps, from the sphere S_0, whose boundaries are $C_{j_1} \cap S_0$.

Consider now the small spherical cap on S_0 cut off by the cone C on which the $2n-1$ truncated cones A_{j_1} sit. We denote by $B_0 \subset S_0$ the region left from this small spherical cap after cutting off the new appeared small spherical cups $\bigcup_{j_1}(C_{j_1} \cap S_0)$.

Then

$$\partial H_1 := \bigcup_{j_1}(A_{j_1} \cup B_{j_1}) \cup P \tag{2.6}$$

is the convex C^1-hypersurface and define H_1 to be the closed, convex ball whose boundary is ∂H_1. Obviously H_1 contains IT_1 and the inner cut locus of ∂H_1 is precisely IT_1.

This construction can be repeated for each segment $s_{j_1 j_2 \cdots j_m} \subset IT$ obtaining in this way a closed, convex ball $H_m \subset \mathbb{R}^n$, which contains IT_m, with C^1-boundary ∂H_m whose (inward) cut locus coincides with the tree IT_m.

Indeed, we construct as follows:

- take a point $\hat{q}_{j_1 j_2 \cdots j_m}$ on the straight line $\gamma_{j_1 j_2 \cdots j_m}$ such that

$$d(q_{j_1 j_2 \cdots j_{m-1}}, \hat{q}_{j_1 j_2 \cdots j_m}) = \frac{r_{m-1}}{\cos(\frac{\phi}{3^m})}; \tag{2.7}$$

- consider the right circular cone $C_{j_1 j_2 \cdots j_m}$ with vertex $\hat{q}_{j_1 j_2 \cdots j_m}$, axis $\gamma_{j_1 j_2 \cdots j_m}$ and vertex angle $\pi - 2\frac{\phi}{3^m}$;
- denote the $(n-1)$-sphere $S_{j_1 j_2 \cdots j_m} := S(q_{j_1 j_2 \cdots j_m}, r_m)$ and consider the spheres $S_{j_1 j_2 \cdots j_m}$ and $S_{j_1 j_2 \cdots j_{m-1}}$ with centers at the ends of the segment $s_{j_1 j_2 \cdots j_m}$.

It follows again that the right circular cone $C_{j_1 j_2 \cdots j_m}$ is exterior tangent to the spheres $S_{j_1 j_2 \cdots j_{m-1}}$ and $S_{j_1 j_2 \cdots j_m}$. The intersection of $C_{j_1 j_2 \cdots j_m}$ with the spheres $S_{j_1 j_2 \cdots j_{m-1}}$ and $S_{j_1 j_2 \cdots j_m}$ is made of the $(n-2)$-spheres $c_{j_1 j_2 \cdots j_{m-1}}$ and $c_{j_1 j_2 \cdots j_m}$, respectively.

Similarly as above, the $(n-2)$-spheres $c_{j_1 j_2 \cdots j_{m-1}}$ and $c_{j_1 j_2 \cdots j_m}$ cut out:

- a truncated cone $A_{j_1 j_2 \cdots j_m} \subset C_{j_1 j_2 \cdots j_m}$;
- a small spherical cap of $S_{j_1 j_2 \cdots j_{m-1}}$ whose boundary is $c_{j_1 j_2 \cdots j_{m-1}} \cap S_{j_1 j_2 \cdots j_{m-1}}$;
- a large spherical cap $S_{j_1 j_2 \cdots j_m}$ whose boundary is $c_{j_1 j_2 \cdots j_m} \cap S_{j_1 j_2 \cdots j_m}$.

Consider now the small spherical cap on $S_{j_1 j_2 \cdots j_{m-1}}$ cut off by the cone $C_{j_1 j_2 \cdots j_m}$ on which the $2n-1$ truncated cones $A_{j_1 j_2 \cdots j_m}$ sit. We denote by $B_{j_1 j_2 \cdots j_m} \subset S_{j_1 j_2 \cdots j_{m-1}}$ the region left from this small spherical cap after cutting off the new appeared small spherical cups $\cup_{j_1 j_2 \cdots j_m}(C_{j_1 j_2 \cdots j_m} \cap S_{j_1 j_2 \cdots j_m})$.

Then

$$\partial H_m := \cup_{i=0}^{m} \cup_{j_1 j_2 \cdots j_m} (A_{j_1 j_2 \cdots j_m} \cup B_{j_1 j_2 \cdots j_m}) \cup P \tag{2.8}$$

is the convex C^1-hypersurface that defines the closed, convex ball H_m in $\mathbb{R}^n$. By a similar argument as above one can see that $\cup_{i=0}^{m} \cup_{j_1 j_2 \cdots j_m} s_{j_1 j_2 \cdots j_m}$ is the inward cut locus of ∂H_m. One can remark that in our construction the conjugate locus coincides with the focal locus.

Indeed, the equal length inward geodesic rays orthogonal to the cloth of the truncated cone $A_{j_1 j_2 \cdots j_m}$, emanating from an arbitrary point of the $(n-2)$-sphere $\{x \in A_{j_1 j_2 \cdots j_m} | d(x, \hat{q}_{j_1 j_2 \cdots j_m}) = \mathit{constant}\}$, concentrate at a point on the open segment $s_{j_1 j_2 \cdots j_m}$. The inward geodesic rays of same length orthogonal to the region $B_{j_1 j_2 \cdots j_m} \subset S_{j_1 j_2 \cdots j_m}$ concentrate at $q_{j_1 j_2 \cdots j_m}$ and similarly the geodesic rays from the large spherical cap of S concentrate at o.

Finally, we define

$$H := \lim_{m \to \infty} H_m \tag{2.9}$$

that have the required properties.

Therefore we obtain

Proposition 2.2. *Let IT be the infinite tree in $\mathbb{R}^n$ and H the closed, convex ball with C^1-boundary constructed above. Then $H \subset \mathbb{R}^n$ contains IT and $E \subset \partial H$ by construction.*

3. The Haussdorff measure of E

In this section we will investigate the Hausdorff dimension of the set E. The idea is to construct a set of points $\hat{E}$ whose Hausdorff dimension $\dim_{\mathcal{H}} \hat{E}$ can be easily computed and such that $\dim_{\mathcal{H}} E = \dim_{\mathcal{H}} \hat{E}$.

We start by defining an infinite series of numbers (α_i), $i \in \{0, 1, \ldots\}$ by

$$\alpha_0 = \frac{3^{k-2}}{3^{k-2} - 1}, \quad \alpha_{i+1} = \frac{1}{3^{k-1}} \alpha_i, \tag{3.1}$$

where t_i is defined in (2.1).

Remark that, for any i, we have

$$\alpha_i = 3\alpha_{i+1} + t_i. \tag{3.2}$$

In $\mathbb{R}^{n-1}$ we consider

- the concentric $(n-2)$-balls $\hat{C} = B(o, \alpha_0)$ and $\hat{S} = B(o, \alpha_0 - t_0)$ with the center o at the origin of $\mathbb{R}^{n-1}$ and radii α_0 and $\alpha_0 - t_0$, respectively;
- $\hat{A} := \hat{C} \setminus \hat{S}$ the annulus obtained by removing $\hat{S}$ from $\hat{C}$.

We will construct a set of points $y_{j_1 j_2 \cdots j_m} \in \hat{S}$, where $m \in \{1, 2, \dots\}$ and $j_m \in \{-(n-1), ..., -1, 0, 1, ..., n-1\}$ are as in Section 2.

For $m = 1$ we consider the points

$$(y_{j_1}) = (y_{-(n-1)}, y_{-(n-2)}, \dots, y_{-2}, y_{-1}, y_0, y_1, y_2, \dots, y_{n-1}) \in \mathbb{R}^{n-1}, \tag{3.3}$$

where

$$\begin{aligned} &(y_1, y_2, \dots, y_{n-1})^t = 2\alpha_1 I_{n-1}, \quad y_0 = o, \\ &(y_{-(n-1)}, y_{-(n-2)}, \dots, y_{-2}, y_{-1})^t = -2\alpha_1 I_{n-1}, \end{aligned} \tag{3.4}$$

where ^{t} represents the transposed of a vector, and I_{n-1} the identity matrix.

We can construct iteratively, for arbitrary m, the set of points $y_{j_1 j_2 \cdots j_m} \in \mathbb{R}^{n-1}$ defined by

$$y_{j_1 j_2 \cdots j_m} = (\sum_{i=1}^{m} 2b_i^1 \alpha_i, \sum_{i=1}^{m} 2b_i^2 \alpha_i, \dots, \sum_{i=1}^{m} 2b_i^{n-1} \alpha_i), \tag{3.5}$$

where (b_i^j) is an $m \times (n-1)$-real matrix defined by

$$b_i^j = \begin{cases} 1, & \text{if } j_i = j \\ -1, & \text{if } j_i = -j \\ 0, & \text{otherwise,} \end{cases} \tag{3.6}$$

for all $i \in \{1, 2, \dots, m\}$ and $j \in \{1, 2, \dots, n-1\}$. One can easily see that for $m = 1$ we get (3.4).

For each m we consider

- the concentric $(n-2)$-balls $\hat{C}_{j_1 j_2 \cdots j_m} = B(o, \alpha_m)$ and $\hat{S}_{j_1 j_2 \cdots j_m} = B(o, \alpha_m - t_m)$;
- $\hat{A}_{j_1 j_2 \cdots j_m} := \hat{C}_{j_1 j_2 \cdots j_m} \setminus \hat{S}_{j_1 j_2 \cdots j_m}$ the annulus obtained by removing $\hat{S}_{j_1 j_2 \cdots j_m}$ from $\hat{C}_{j_1 j_2 \cdots j_m}$ (see Figs. 4, 5 for the case $n = 3$).

Let us denote the set of all points y by $Y := \cup_{m=1}^{\infty} y_{j_1 j_2 \cdots j_m}$, and let $\hat{E}$ be the set of accumulation points of Y. Since $Y \subset \hat{S}$ the set of points $\hat{E} \subset \hat{S}$ exists and it is not empty.

Let $\hat{R}_1 : \mathbb{R}^{n-1} \to \mathbb{R}^{n-1}$ be the contraction function that maps $\hat{S}$ into $\hat{S}_1$. It can be seen that $\hat{R}_1$ is a *similarity map*, i.e. there exists a constant $c_1 \in (0, 1)$ such that

$$d(\hat{R}_1(x), \hat{R}_1(y)) = c_1 d(x, y), \tag{3.7}$$

for any $x, y \in \mathbb{R}^{n-1}$. The constant c_1 is called the *ratio* of $\hat{R}_1$ (see [4], p. 128). Indeed, taking into account our definitions, one obtains $c_1 = \dfrac{1}{3^{k-1}}$.

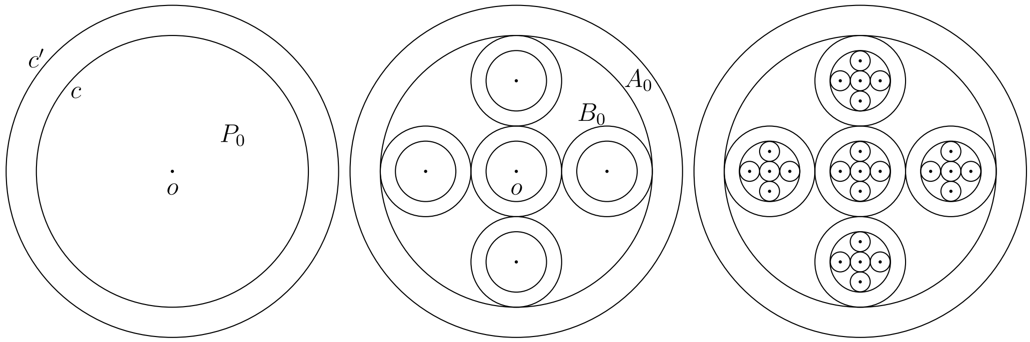

Fig. 4. Mandalas seen from a far point on the ray γ in the cases $IT_0 = s$ (left), $IT_1 = \{s, s_{j_1} | j_1 \in \{-2, -1, 0, 1, 2\}\}$ (middle) and $IT_2 = \{s, s_{j_1}, s_{j_1 j_2} | j_i \in \{-2, -1, 0, 1, 2\}, i = 1, 2\}$ (right).

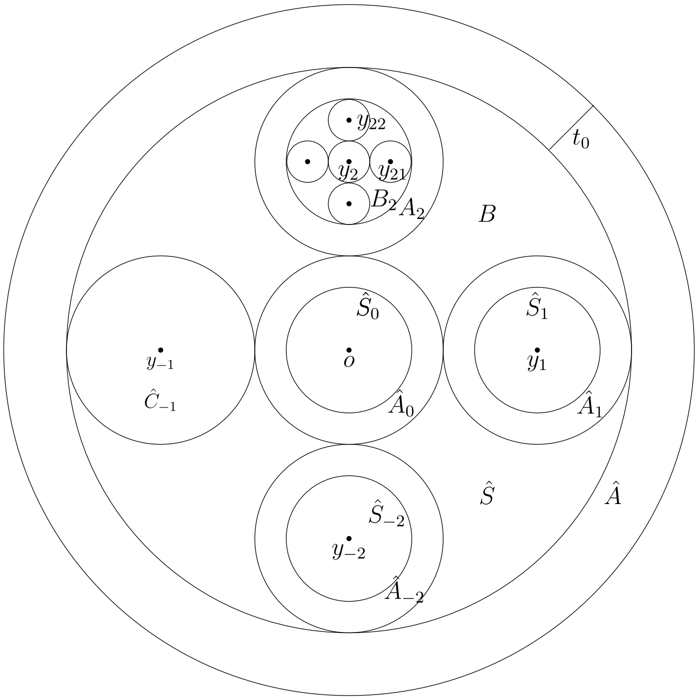

Fig. 5. A combined mandala seen from a far point on the ray γ.

Iteratively, for a given m, we define the mapping

$$\hat{R}_j : \mathbb{R}^{n-1} \to \mathbb{R}^{n-1}, \quad \hat{S}_{j_1 j_2 \cdots j_m} \mapsto \hat{S}_{j_1 j_2 \cdots j_m} j, \tag{3.8}$$

for all $j \in \{-(n-1), ..., -1, 0, 1, ..., n-1\}$. Obviously $\hat{R}_j$ is a similarity map with ratio $c_j = \dfrac{1}{3^{k-1}}$. Thus each $\hat{R}_j$ transform subsets of $\mathbb{R}^{n-1}$ into geometrically similar sets.

The attractor of such a collection of similarity maps values domains, in our case $\hat{E}$, is a *self-similar set*, being a union of smaller similar copies of itself.

We recall from [4] that the mappings $\hat{R}_j$ satisfy the *open set condition* if there exists a non-empty bounded open set V such that

$$V \supset \bigcup_{j=1}^{2n-1} \hat{R}_j(V). \tag{3.9}$$

By taking $V := \hat{S}$ one can see that the mappings $\hat{R}_j$ considered in (3.8) satisfy the open set condition.

It follows from Theorem 9.3 in [4] that the Hausdorff dimension $s := \dim_H \hat{E}$ can be computed from the formula

$$\sum_{j=1}^{2n-1} (c_j)^s = 1, \tag{3.10}$$

where c_j are the ratios of the similarity maps $\hat{R}_j$. Therefore, in our case we have

$$\sum_{j=1}^{2n-1} \left(\frac{1}{3^{k-1}}\right)^s = 1, \tag{3.11}$$

and by an elementary computation we obtain

$$s = \frac{\log(2n-1)}{(k-1)\log 3}. \tag{3.12}$$

Imposing now the condition $1 < s < 2$ we get

$$\frac{3^{k-1}}{2} < n < \frac{3^{2(k-1)}+1}{2}, \tag{3.13}$$

where n and k are positive integers. A moment of thought convinces that

$$n = \frac{3^{k-1}+3}{2} \tag{3.14}$$

is a positive integer that satisfies this condition (n is obviously integer because all powers of an odd number are odd and sum of two odd numbers is even).

Therefore, we have

Proposition 3.1. *Let $k \geq 2$ be a fixed integer and let $n := \frac{3^{k-1}+3}{2}$. Then*

$$\dim_H \hat{E} = \frac{\log(2n-1)}{(k-1)\log 3} \in (1,2), \tag{3.15}$$

where $\hat{E}$ is the accumulation points set of Y constructed as above.

Remark that the minimal admitted value for n is $n = 3$ for $k = 2$. In this case we have $\dim_H \hat{E} = \frac{\log 5}{\log 3} = 1.46497$.

Let us point out that the sets $\hat{S}$ and $H = \cup_{m=0}^{\infty} \cup_{j_1 j_2 \cdots j_m} A_{j_1 j_2 \cdots j_m} \cup B_{j_1 j_2 \cdots j_m}$ are bi-Lipschitz, i.e. one can define a map $\Phi : \hat{S} \to H$ and there are positive constants c and C such that

$$c \cdot d(x,y) \leq d(\Phi(x), \Phi(y)) \leq C \cdot d(x,y), \tag{3.16}$$

for all $x, y \in \hat{S}$. Indeed, since ϕ has been chosen arbitrary, if we take a small $\phi < \varepsilon$, for any $\varepsilon > 0$, then $\frac{\pi}{2} - \phi \to \frac{\pi}{2}$, i.e. the small spherical caps $S_{j_1 j_2 \cdots j_m}$ are almost included in the orthogonal planes to the rays $\gamma_{j_1 j_2 \cdots j_m}$. This means that $\hat{S}$ and H are bi-Lipschitz.

On the other hand, it is known that the Hausdorff dimensions of two bi-Lipschitz sets coincide (see [4] for example), and therefore we obtain

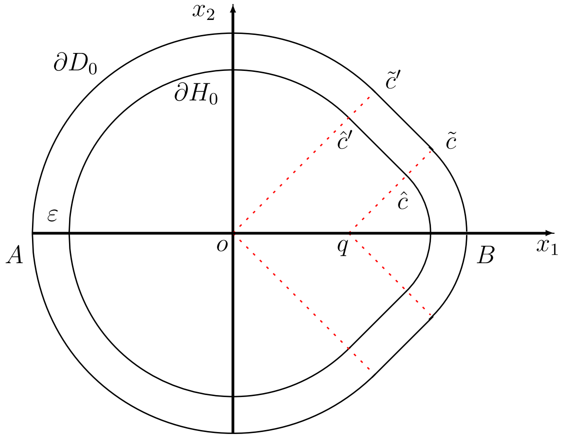

Fig. 6. The ε-dilatation of the convex ball H_0.

Corollary 3.2. *Let $k \geq 2$ be a fixed integer and let $n := \frac{3^{k-1}+3}{2}$. Then*

$$\dim_H E = \frac{\log(2n-1)}{(k-1)\log 3} \in (1, 2), \tag{3.17}$$

where E is the set of endpoints of IT constructed in Section 2.

We point out that the dimension $n(k)$ increases exponentially with k.

4. Proof of Theorem 1.1

In this section we construct a closed, convex ball in $\mathbb{R}^n$ such that the inward cut locus of ∂D coincides with the infinite tree IT. Then we will smooth out the truncated cones $A_{j_1 j_2 \cdots j_m}$ at each depth level m.

Firstly, for each depth level m, let us consider an "ε-dilatation" of the closed, convex ball H_m, namely we define

$$D_m := \{\text{the convex ball whose boundary is } \partial H_m\} \cup \{x \in \mathbb{R}^n \mid d(x, \partial H_m) \leq \varepsilon\}, \tag{4.1}$$

for any positive constant $\varepsilon > 0$. Denote the limit

$$D := \lim_{m\to\infty} D_m \tag{4.2}$$

that is the ε-dilatation of convex ball H.

Note that the boundary $\partial D \in \mathbb{R}^n$ is the convex C^1-hypersurface

$$\partial D = \lim_{m\to\infty} \left[\cup_{i=0}^{m} \cup_{j_1 j_2 \cdots j_m} (\tilde{A}_{j_1 j_2 \cdots j_m} \cup \tilde{B}_{j_1 j_2 \cdots j_m})\right] \cup \tilde{P} \cup \tilde{E}, \tag{4.3}$$

where the tilde notation means the ε-dilatation of the corresponding geometrical objects of H.

One can easily see that the geodesics orthogonal to ∂D are in fact geodesics to H extended by ε at one of their ends, and therefore the inward cut locus of ∂D coincides with the infinite tree IT. Obviously the set of end points E are now in the interior of the ball D and not on its boundary as in the case of H. This allows us to realize the infinite tree IT as the inward cut locus of a hypersurface in $\mathbb{R}^n$.

Secondly, we are going to smooth out the truncated cones $\tilde{A}_{j_1 j_2 \cdots j_m}$ on ∂D such that the inward cut locus does not change.

Let us refer to Fig. 6 restricted to the upper half Euclidean plane $\mathbb{H} := \{(x_1, x_2) \in \mathbb{R}^2 \mid x_2 > 0\}$. Recall that S and S_0 are circles of centers o and q with radii r_{-1} and r_0, respectively. We further denote:

- the intersection points of ∂D_0 with the horizontal coordinate axis by $A(a, 0)$ and $B(b, 0)$, $a < b$, respectively;
- the x_1 coordinates of the points $\tilde{c}'$ and $\tilde{c}$ by t_1 and t_2;
- the straight line segment determined by the points $\tilde{c}'$ and $\tilde{c}$ by $d = \{d(x_1) \mid t_1 < x_1 < t_2\}$.
- the large circular segment on ∂D_0 from A to $\tilde{c}'$ by $\{f_1(x_1) \mid a < x_1 < t_1\}$, and the small circular segment on ∂D_0 from $\tilde{c}$ to B by $\{f_2(x_1) \mid t_2 < x_1 < b\}$.

We have the following smoothing Proposition:

Proposition 4.1. *With the notations above, there is a C^∞-function $F(x_1)$ defined on $[a, b]$ that takes values in $\mathbb{H}$ such that*

- *$F(x_1) = f_1(x_1)$ for $x_1 \in [a, t_1]$;*
- *$F(x_1) = f_2(x_1)$ for $x_1 \in [t_2, b]$;*
- *$d(x_1) \geq F(x_1) \geq \max(f_1(x_1), f_2(x_1))$, for $t_1 < x_1 < t_2$;*
- *all the inward straight lines (geodesic rays) orthogonal to $F(x_1)$, for $t_1 < x_1 < t_2$, do not intersect each other in the region $\{x_2 < d(x_1)\} \cap \mathbb{H}$.*

In other words, we will contract a smooth curve that joins points $\tilde{c}'$ and $\tilde{c}$. By the same operation in the lower half plane $\{(x_1, x_2) \mid x_2 \leq 0\}$ we obtain a smooth plane curve.

Proof. For the sake of simplicity we rotate counterclockwise with $\frac{\pi}{2} - \phi$ the coordinates system used in Section 2 (compare with Fig. 2) obtaining Fig. 7 (left). The new coordinate system is denoted with $\{x, y\}$ while $\tilde{c}'$, $\tilde{c}$, f_1, f_2, d have the same meaning as above. We denote the coordinates of points $\tilde{c}'$ and $\tilde{c}$ by $(x_{\tilde{c}'}, y_{\tilde{c}'})$ and $(x_{\tilde{c}}, y_{\tilde{c}})$, respectively. Moreover, we denote $\{R\} = f_1 \cap f_2$ with coordinates (x_R, y_R). In Fig. 7 we have expressed by vertical dots the fact that y_R is actually quite far from the origin o and quite closed to $\tilde{c}'$, i.e. $d(o, y_R) >> d(y_R, y_{\tilde{c}'})$.

With these notations, we consider the function

$$F_1(x) := \int_0^x [1 - g_\sigma(t)] f_1'(t) dt|_{\sigma=x} + y_{\tilde{c}'}, \qquad 0 \leq x \leq x_R, \tag{4.4}$$

where $0 < \sigma \leq x_R$,

$$g_\sigma(t) := \begin{cases} 0, & t \leq 0 \\ \frac{\varphi(t)}{\varphi(t)+\varphi(\sigma-t)}, & 0 < t < \sigma \\ 1, & t \geq \sigma \end{cases} \tag{4.5}$$

and

$$\varphi(t) := \begin{cases} 0, & t \leq 0 \\ e^{-\frac{1}{t}}, & t > 0. \end{cases} \tag{4.6}$$

It is elementary to see that F_1 is a smooth monotone non-increasing function on $[0, x_R]$, $F_1(x) \geq f_1(x)$, $F_1(0) = x_{\tilde{c}'}$, $F_1(x_R) = y_R + \delta_1$, $\delta_1 > 0$. Moreover $F_1'(0) = 0 = F_1'(x_R)$.

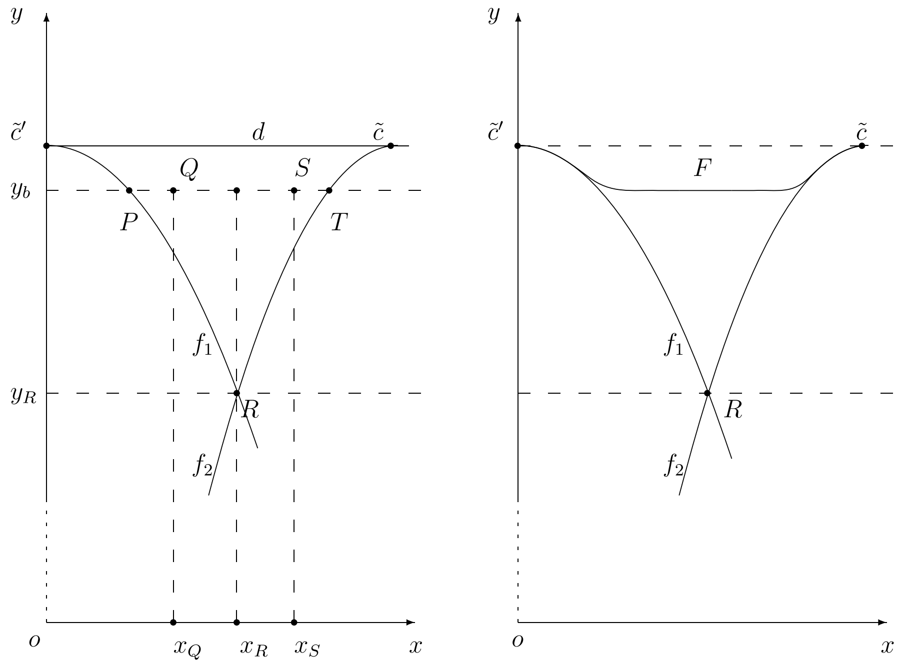

Fig. 7. Smoothing of ∂D_0. Before smoothing (left), after smoothing (right).

Similarly, we define

$$F_2(x) := \int_x^1 h_\rho(t) f_2'(t) dt|_{\rho=x} + y_{\tilde{c}}, \qquad x_R \leq x \leq x_{\tilde{c}}, \tag{4.7}$$

where $x_R < \sigma \leq x_{\tilde{c}}$,

$$h_\rho(t) := \begin{cases} 1, & t \leq 0 \\ \frac{\varphi(t-\rho)}{\varphi(t-\rho)+\varphi(1-t)}, & 0 < t < \rho \\ 0, & t \geq \rho \end{cases} \tag{4.8}$$

and φ same as above.

One can easily see that F_2 is a smooth monotone non-decreasing function on $[x_R, x_{\tilde{c}}]$, $F_2(x) \geq f_2(x)$, $F_2(x_R) = y_R + \delta_2$, $\delta_2 > 0$, $F_2(x_{\tilde{c}}) = y_{\tilde{c}}$. Moreover $F_2'(x_R) = 0 = F_2'(x_{\tilde{c}})$.

It is obvious that we can choose now a constant $y_b \in (\max\{y_R + \delta_1, y_R + \delta_2\}, y_{\tilde{c}})$, in practice y_b will be taken as closed as possible to $y_{\tilde{c}'}$, such that there exists $x_Q \in (0, x_R)$ and $x_S \in (x_R, x_{\tilde{c}})$ that satisfies $F_1(x_Q) = F_2(x_S) = y_b$ (see Fig. 7).

With these, we redefine

$$F_1(x) := \int_0^x [1 - g_{x_Q}(t)] f_1'(t) dt + y_{\tilde{c}'}, \qquad 0 \leq x \leq x_Q, \tag{4.9}$$

and

$$F_2(x) := \int_x^1 h_{x_S}(t) f_2'(t) dt + y_{\tilde{c}}, \qquad x_S \leq x \leq x_{\tilde{c}}. \tag{4.10}$$

Then the function

$$F(x) := \begin{cases} F_1(x), & 0 \leq x \leq x_Q \\ y_b, & x_Q < x < x_S \\ F_2(x), & x_S \leq x \leq x_{\tilde{c}} \end{cases} \tag{4.11}$$

will have the required properties.

One can see that the curvature of F_1, namely $k_{F_1}(x) := \frac{F_1''}{[1+(F_1')^2]^{3/2}}$, satisfies $k_{f_1} \leq k_{F_1}$ on $[0, x_{\tilde{c}}]$ and similar for F_2. This guaranties that F smoothly joins points $\tilde{c}'$ and $\tilde{c}$ and that the inner normals to F cannot intersect each other in the region $[0, x_{\tilde{c}}] \cap \mathbb{H}$. □

We denote by $\tilde{D}_0$ the ball obtained from D_0 after smoothing out the truncated cones making use of the function F introduced in Proposition 4.1. D_0 is actually a surface of revolution obtained by rotating the profile curve $F_1([a, t_1]) \cup F_2([t_2, b]) \cup d((t_1, t_2))$ around the γ axis. This is a C^∞-surface whose inward cut locus is the segment oq.

This construction can be repeated in any dimension, we apply the above smoothing procedure to each ∂D_m, inductively. In this way we end up with a ball $\widetilde{D}_m \subset \mathbb{R}^n$ with C^∞ boundary.

By putting

$$\widetilde{D} := \lim_{m\to\infty} \widetilde{D}_m \tag{4.12}$$

we obtain a closed, convex ball in $\mathbb{R}^n$ with boundary $\partial\widetilde{D}$ such that the inward cut locus of $\partial\widetilde{D}$ is the infinite tree IT, actually a fractal as shown in Section 3.

One should remark that the set of end points E of the fractal IT are in the interior of $\widetilde{D}$ at distance ε from the hypersurface $\partial\widetilde{D}$. However, taking into account that these end points actually lie on the tree branches $\gamma_{j_1 \dots j_m}$, by extending these branches, they will intersect $\partial\widetilde{D}$ giving a set of points $\widetilde{E}$ on $\partial\widetilde{D}$. Such a point is the point B in Fig. 6, for $m = 0$. We point out that the points $\widetilde{E}$ are on $\partial\widetilde{D}$, but they do not belong to the fractal IT, they are only an ε-displacement of the end points E.

We will study in the following the differentiability of $\partial\widetilde{D}$. We have

Proposition 4.2. *The hypersurface $\partial\widetilde{D}$ in $\mathbb{R}^n$ is:*

1. *at least k-differentiable at points $\widetilde{E}$,*
2. *C^∞ at any point $\partial\widetilde{D} \setminus \widetilde{E}$.*

Proof. Let us denote

$$\widetilde{q}_{j_1 j_2 \dots j_m} := \partial\widetilde{D}_m \cap \gamma_{j_1 j_2 \dots j_m}, \qquad \widetilde{Q} := \bigcup_{m=1}^{\infty} \{q_{j_1 j_2 \dots j_m}\}. \tag{4.13}$$

It can be seen that $\widetilde{E}$ is the set of accumulation points of $\widetilde{Q}$. A moment of thought shows that the set $\partial\widetilde{D}_m \cap \partial\widetilde{D}_{m-1}$ is a circle on the sphere $S(q_{j_1 j_2 \dots j_{m-1}}, r_{m-1} + \varepsilon)$, namely the base of the spherical cap cut off by the smoothed truncated cone $\widetilde{A}_{j_1 j_2 \dots j_m}$, and that $\widetilde{q}_{j_1 j_2 \dots j_{m-1}} = S(q_{j_1 j_2 \dots j_{m-1}}, r_{m-1} + \varepsilon) \cap \gamma_{j_1 j_2 \dots j_m}$. Obviously $\widetilde{E}$ is not countable.

We define the function

$$\zeta : \bigcup_{m=1}^{\infty} \partial\widetilde{D}_{m-1} \to (0, \infty), \quad \zeta(\widetilde{q}_{j_1 j_2 \dots j_{m-1}}) = d(\widetilde{q}_{j_1 j_2 \dots j_m \dots \infty}, \widetilde{q}_{j_1 j_2 \dots j_{m-1}}), \tag{4.14}$$

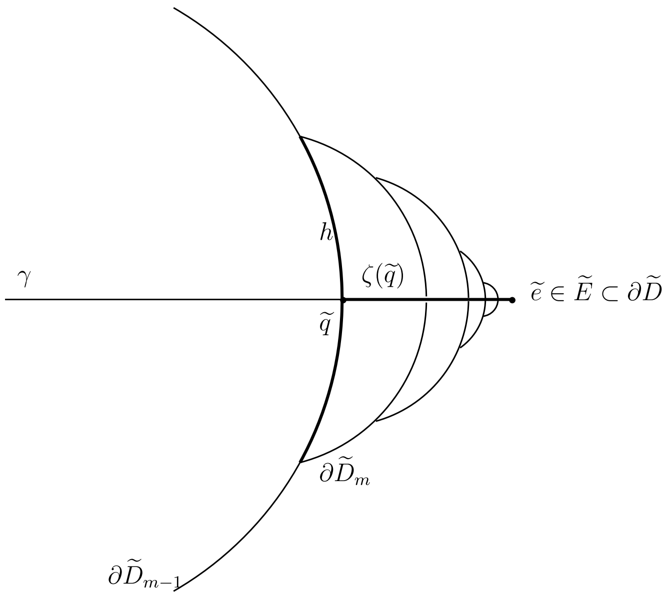

Fig. 8. The function ζ. For simplicity we have denoted $\gamma := \gamma_{j_1 j_2 \dots j_{m-1}}$, $\widetilde{q} := \widetilde{q}_{j_1 j_2 \dots j_{m-1}}$ and $\widetilde{e} := \widetilde{q}_{j_1 j_2 \dots j_m \dots \infty}$ (the smoothing function F is not drawn).

where $\widetilde{q}_{j_1 j_2 \dots j_m \dots \infty} \in \widetilde{E}$ (see Fig. 8).

One can see that the differentiability of $\partial\widetilde{D}$ at points of $\widetilde{E}$ can be expressed in terms of the differentiability of ζ. Indeed, let $A \in \partial\widetilde{D}$ be a point such that there is an m for which $A \in \partial\widetilde{D}_{m-1}$ and denote by $\mathfrak{r}(u^1, u^2, \dots, u^{n-1})$ its position vector in $\mathbb{R}^n$, when we denote by $(u^1, u^2, \dots, u^{n-1})$ the local coordinates on $\widetilde{D}$. Likely, let $B \in \partial\widetilde{D}$ be a point such that $B \in \partial\widetilde{D}_m$ with position vector $\Phi(u^1, u^2, \dots, u^{n-1}) \in \mathbb{R}^n$. Then it is clear that

$$\Phi(u^1, u^2, \dots, u^{n-1}) = h(u^1, u^2, \dots, u^{n-1}) \cdot \mathfrak{e}(u^1, u^2, \dots, u^{n-1}) + \mathfrak{r}(u^1, u^2, \dots, u^{n-1}), \tag{4.15}$$

where $\mathfrak{e}(u^1, u^2, \dots, u^{n-1})$ is the outward pointing unit normal vector to $\partial\widetilde{D}_{m-1}$ at A, and h is the height function $h(u^1, u^2, \dots, u^{n-1}) = d(A, B)$. Here d is the usual Euclidean distance. Then we can see that $h|_{\widetilde{E}} = \zeta|_{\widetilde{E}}$.

Obviously Φ is C^∞ at any point $\widetilde{D} \setminus \widetilde{E}$ by construction, so we need to investigate only the differentiability of $\zeta|_{\widetilde{E}}$.

Let us recall that the r differential of ζ can be written using finite differences as follows

$$\frac{d^r \zeta}{dx^r} = \lim_{h \to 0} \frac{\delta_h^r[\zeta]}{h^r}, \quad r \geq 1 \tag{4.16}$$

where

$$\delta_h^r[\zeta] := \sum_{i=0}^{r} (-1)^i \binom{r}{i} \zeta\Big(x + \Big(\frac{r}{2} - i\Big)h\Big) \tag{4.17}$$

and $h = d(\partial\widetilde{D}_m \cap \partial\widetilde{D}_{m-1}, \widetilde{q}_{j_1 j_2 \dots j_{m-1}})$.

Let us remark that

$$\begin{aligned}\frac{\delta_h^r[\zeta]}{h^r} &\leq \frac{2^{k-1}}{h^r} d(\max\zeta, \min\zeta) = \frac{2^{k-1}}{h^r} d(\widetilde{q}_{j_1 j_2 \dots j_m \dots \infty}, \widetilde{q}_{j_1 j_2 \dots j_{m-1}}) \\ &= \frac{2^{k-1}}{h^r} \sum_{i=0}^{\infty} d(\widetilde{q}_{j_1 j_2 \dots j_m}, \widetilde{q}_{j_1 j_2 \dots j_{m-1}})\end{aligned} \tag{4.18}$$

On the other hand, we compute

$$h = d(\partial\widetilde{D}_m \cap \partial\widetilde{D}_{m-1}, \widetilde{q}_{j_1 j_2 \dots j_{m-1}}) = \varphi\Big(\frac{1}{3}\Big)^{m-1}(r_{m-1}+\varepsilon) > \phi\Big(\frac{1}{3}\Big)^m (r_{m-1}+\varepsilon), \tag{4.19}$$

and

$$\begin{aligned}d(\widetilde{q}_{j_1 j_2 \dots j_m}, \widetilde{q}_{j_1 j_2 \dots j_{m-1}}) &= (r_m+\varepsilon) - (r_{m-1}+\varepsilon) + l_m = l_m\Big(1 - \cos\phi\Big(\frac{1}{3}\Big)^m\Big) \\ &= \frac{1}{(3^{k-1})^m} \tan\Big(\frac{1}{2}\phi\Big(\frac{1}{3}\Big)^m\Big),\end{aligned} \tag{4.20}$$

where we have used $r_m - r_{m-1} = -l_m \cos\phi\left(\frac{1}{3}\right)^m$, and the well known trigonometric formula $\dfrac{1-\cos\eta}{\sin\eta} = \tan\frac{\eta}{2}$.

One can easily see that there are infinitely many terms in the sum in the right hand side of the last equality in (4.18), therefore, there is no harm in leaving out a finite number of them, say the first $m-1$ terms. It follows

$$d(\widetilde{q}_{j_1 j_2 \dots j_m \dots \infty}, \widetilde{q}_{j_1 j_2 \dots j_{m-1}}) = \sum_{i=m}^{\infty} \frac{1}{(3^{k-1})^i} \tan\Big(\frac{1}{2}\phi\Big(\frac{1}{3}\Big)^i\Big) = \sum_{i=m}^{\infty} \frac{1}{(3^{k-1})^i} \Big(\frac{1}{2}\phi\Big(\frac{1}{3}\Big)^i\Big) = \frac{\phi}{2}\frac{1}{3^{km-1}} \tag{4.21}$$

where we have used the well-known formula $\lim_{\tau\to 0} \dfrac{\tan\tau}{\tau} = 1$.

Let us remark now that $h \to 0$ when $m \to \infty$ by construction, so there is no harm in regarding $\lim_{h\to 0}$ as $\lim_{m\to\infty}$.

It results

$$\lim_{h\to 0} \frac{\delta_h^r[\zeta]}{h^r} \leq \lim_{m\to\infty} \frac{\frac{\phi}{2}\frac{1}{3^{km-1}}}{\Big[\phi\Big(\frac{1}{3}\Big)^m (r_{m-1}+\varepsilon)\Big]^r} = \frac{1}{2}\lim_{m\to\infty}\Big[\frac{1}{\phi^{r-1}(r_{m-1}+\varepsilon)^r} \times \frac{1}{3^{mk-r(m-1)}}\Big] \tag{4.22}$$

One can now easily see that in the case $r = k$ the limit in the right hand side of (4.22) takes the finite value $\dfrac{1}{2}\dfrac{1}{3^k}\dfrac{1}{\phi^{k-1}\varepsilon^k}$ and therefore $\lim_{h\to 0}\frac{\delta_h^r[\zeta]}{h^r}$ is finite at a point of $\widetilde{E}$, hence the function ζ is at least k-differentiable on $\widetilde{E}$. Remark that for $r < k$, (4.22) implies $\dfrac{d^r\zeta}{dx^r} = 0$, namely $\partial\widetilde{D}$ is C^{k-1} everywhere, while for $r > k$ we cannot say anything about the convergence of the limit in the left hand side of (4.22).

The proposition is proved. □

In order to finish our construction, we adapt an idea of A. Weinstein from [15], namely the technique of *making any disc a unit disc*. We have

Proposition 4.3. *Let Δ be an n-dimensional ball embedded in a C^r manifold M of dimension n. For any Riemannian metric on $M \setminus$(interior of Δ), there is a new Riemannian on M, agreeing with the original metric* *on $M \setminus$ (interior of Δ), such that for some point $p \in \Delta$ the exponential map exp_p is a C^r diffeomorphism of the unit ball around the origin in T_pM onto Δ.*

This proposition can be proved by exactly the same method as Theorem C in [15].

We reach the final stage of our construction.

Recall that an n-sphere $\mathbb{S}^n$ can be always constructed topologically by gluing together the boundaries of a pair of n-balls (Δ_1, Δ_2) provided they have opposite orientations. The boundary of an n-ball Δ_i is an $(n-1)$-sphere $\partial\Delta_i \simeq \mathbb{S}^{n-1}$, and these two $(n-1)$-spheres are to be identified, for $i = 1, 2$.

In other words, if we have a pair of n-balls of the same size, we superpose them so that their $(n-1)$-spherical boundaries match, and let matching pairs of points on the pair of $(n-1)$-spheres be identically equivalent to each other $\partial\Delta_1 \equiv \partial\Delta_2$. In analogy with the case of the 2-sphere, the gluing surface, that is an $(n-1)$-sphere subset of $\mathbb{S}^n$, can be called "equatorial sphere". Obviously, the interiors of the original n-balls are not glued to each other but they cover the "exterior" surface of $\mathbb{S}^n = \Delta_1 \bigcup \Delta_2$.

Keeping this topological construction in mind, we will glue together the n-ball $\widetilde{D}$ constructed above with a new n-dimensional ball Δ by identifying $\partial\Delta$ with the hypersurface H through a C^k diffeomorphism. By this construction we obtain an n-sphere $\mathbb{S}^n$ whose equatorial sphere is $\partial\Delta \equiv \partial\widetilde{D} \simeq \mathbb{S}^{n-1}$. Moreover, the infinite tree $IT \subset \widetilde{D}$ lies down on the surface $\mathbb{S}^n$, more precisely, in the open region cut off by the equatorial sphere and covered by the interior of $\widetilde{D}$. By construction, all the cut points of IT are at a certain distance (the ε-dilatation) from the equatorial sphere. Therefore, $IT \subset \mathbb{S}^n$, but $IT \cap \bar{\Delta} = \emptyset$, where $\bar{\Delta}$ is the closure of Δ.

Finally, by applying the Proposition 4.3 to this n-sphere $M = \mathbb{S}^n$, in the case $r = k-1$ with the supplementary condition of k-differentiability (see Proposition 4.2), and asking $n = \frac{3^{k+1}}{2} + 1$, we obtain a new Riemannian metric g on $\mathbb{S}^n$, metric that coincides on $\mathbb{S}^n \setminus$ (*interior of* Δ) with the initial flat metric defined on $\widetilde{D}$, and a point $p \in$ (*interior of* Δ) $\subset \mathbb{S}^n$ whose cut locus is IT. Obviously, the geodesics of (M, g) starting from p must cross the equatorial sphere before hitting the cut locus IT.

Of course, this Riemannian structure cannot be C^∞ because this would contradict with the main result in [8], namely that the Hausdorff dimension of the cut locus of any point on a C^∞ Riemannian manifold must be an integer.

Also we remark that $k \to \infty$ would lead to $n \to \infty$ and hence our n-sphere must be infinite dimensional, but this is not allowed (see Proposition 3.1 and Corollary 3.2).

The Theorem 1.1 is now proved.

5. Randers metrics: a ubiquitous family of Finsler structures

Let us recall that a *Finsler manifold* (M, F) is a n-dimensional differential manifold M endowed with a norm $F : TM \to [0, \infty)$ such that F is 1-positive homogeneous, i.e. $F(x, \lambda y) = \lambda F(x, y)$, for $\lambda > 0$, $(x, y) \in TM$, and the Hessian matrix $g_{ij}(x, y) := \dfrac{1}{2}\dfrac{\partial^2 F^2}{\partial y^i \partial y^j}$ is positive definite on $\widetilde{TM} := TM \setminus \{0\}$.

The Finsler structure is called *absolute homogeneous* if $F(x, -y) = F(x, y)$ because this leads to the homogeneity condition $F(x, \lambda y) = |\lambda| F(x, y)$, for any $\lambda \in \mathbb{R}$.

Let $\gamma : [a, b] \to M$ be a regular piecewise C^∞ curve in M, and let $a := t_0 < t_1 < \cdots < t_k := b$ be a partition of $[a, b]$ such that $\gamma_{|[t_{i-1}, t_i]}$ is smooth for each interval $[t_{i-1}, t_i]$, $i \in \{1, 2, \dots, k\}$. The *integral length* of γ is given by

$$L(\gamma) := \sum_{i=1}^{k} \int_{t_{i-1}}^{t_i} F(\gamma(t), \dot{\gamma}(t)) dt, \tag{5.1}$$

where $\dot{\gamma} = \dfrac{d\gamma}{dt}$ is the tangent vector along the curve $\gamma_{|[t_{i-1}, t_i]}$.

A regular C^∞ piecewise curve γ on a Finsler manifold is called a *geodesic* if $L'(0) = 0$ for all piecewise C^∞ variations of γ that keep its end points fixed.

For any two points p, q on M, let us denote by $\Omega_{p,q}$ the set of all piecewise C^∞ curves $\gamma : [a, b] \to M$ such that $\gamma(a) = p$ and $\gamma(b) = q$. The map

$$d : M \times M \to [0, \infty), \qquad d(p, q) := \inf_{\Omega_{p,q}} L(\gamma) \tag{5.2}$$

gives the *Finslerian distance* on M. It can be easily seen that d is in general a quasi-distance, i.e. it has the properties

1. $d(p, q) \geq 0$, with equality if and only if $p = q$;
2. $d(p, q) \leq d(p, r) + d(r, q)$, with equality if and only if p, q, r are on the same geodesic segment (triangle inequality).

In the case when (M, F) is absolutely homogeneous, the symmetry condition $d(p, q) = d(q, p)$ holds and therefore (M, d) is a genuine metric space. We do not assume this symmetry condition in the present paper.

A Randers metric on an n-differential manifold M is a special Finsler metric $(M, F := \alpha + \beta)$ obtained by a deformation of a Riemannian metric $a := a_{ij}(x)dx^i \otimes dx^j$ by a one-form $\beta := b_i(x)dx^i$. The resulting Finslerian norm $F : TM \to [0, \infty)$ is given by

$$F(x, y) := \alpha(x, y) + \beta(x, y) = \sqrt{a_{ij}(x)y^i y^j} + b_i(x)y^i, \quad (x, y) \in TM. \tag{5.3}$$

It is well known that imposing the condition $b^2 := a(b, b) < 1$ is enough to ensure that this F is a positive definite Finsler structure in the usual sense (see [1] for details).

The following results are well known (see [1]):

Proposition 5.1. *Let $(M, F = \alpha + \beta)$ be a Randers space. The 1-form β is closed if and only if the geodesics of the Randers metric F coincide with the geodesics of the underlying Riemannian structure as point sets.*

In other words, the Randers space $(M, F = \alpha + \beta)$ has reversible geodesics (see [11] for details).

Corollary 5.2. *Let (M, α) be a Riemannian space form and β a 1-form on M. The 1-form β is closed if and only if the Randers metric $(M, F = \alpha + \beta)$ is projectively flat.*

Remark 5.3. The Randers metrics can be described as the deformation of the Riemannian metric a by means of a magnetic field specified by the 1-form β.

5.1. A Randers metric on the n-ball $\mathcal{B}^n$

Let us consider the 2-ball $\mathcal{B}^2 := \{(x, y) \ |(x, y)| \leq 1\} \subset \mathbb{R}^2$, where $|\cdot|$ is the usual Euclidean norm, and introduce the usual polar coordinates (r, θ).

We will denote the coordinates of that tangent space at a point to $\mathcal{B}^2$ by $(r, \theta; x, y) \in T\mathcal{B}^2$ regarding (r, θ) as coordinates on the base manifold $\mathcal{B}^2$ and $(x, y) \in T_{(r,\theta)}\mathcal{B}^2$ the fiber coordinates.

The inward geodesics with the start point on the 2-ball $\mathcal{B}^2$ endowed with the Euclidean metric are rays that gather in the origin $O \in \mathbb{R}^2$ and since are all Euclidean unit length, the inward cut locus of the boundary $\partial\mathcal{B}^2 = \mathbb{S}^1$ is O.

We are going to construct a magnetic field $\beta = b_1(r, \theta)dr + b_2(r, \theta)d\theta$ acting along the inward rays α-orthogonal to the boundary $\partial\mathcal{B}^2$. Moreover, we will ask for this magnetic field to vanish at both ends of the inward rays.

Lemma 5.4. *There exists an even, non-constant C^∞ function $h : [-1, 1] \to [0, 1)$ such that $h(-1) = 0 = h(1)$.*

Proof. Choose any constants $c \in (0, 30.05)$ and $\delta \in (0, 1)$.

The function

$$h(x) = \begin{cases} 0, & -1 \leq t \leq -\delta \\ cg(\frac{t}{\delta} + 2)g(-\frac{t}{\delta} + 2), & -\delta < t < \delta \\ 0, & \delta \leq t \leq 1 \end{cases} \tag{5.4}$$

has the desired properties, where g is the function

$$g : (-3, 3) \setminus \{0, 1] \to [0, 1], \qquad g(t) := \frac{\varphi(t)}{\varphi(t) + \varphi(1 - t)}, \tag{5.5}$$

and φ is as in (4.6). $\square$

Remark 5.5. The function h in Lemma 5.4 can be actually defined on any finite interval $[a, b] \subset \mathbb{R}$ and extended to a function $h : [a, b] \to [0, 1)$ with $h(a) = h(b) = 0$.

We consider the magnetic field defined by the 1-form $\beta = b_1(r, \theta)dr + b_2(r, \theta)d\theta$ given by

$$b_1 = h(r), \qquad b_2 = 0 \tag{5.6}$$

where $h : [0, 1] \to [0, 1)$ is a function constructed as shown in Lemma 5.4.

Then we have

Proposition 5.6.

1. *The fundamental function $F = \alpha + \beta$, where α is given by the Euclidean metric in polar coordinates and $\beta = h(r)dr$, is a positive definite Randers metric on $\mathcal{B}^2$.*
2. *The Randers metric $(\mathcal{B}^2, F)$ is projectively flat.*
3. *The cut locus of the boundary $\partial\mathcal{B}^2$ with respect to the Randers metric is the origin O.*

Proof.

1. Remark that $b = h(r) < 1$ and therefore F is a positive definite Randers metric.
2. Moreover, the 1-form β is closed by construction, therefore the Randers geodesics coincide with the underlying Riemannian geodesics as set of points and the second statement follows.
3. For the last statement, we remark that near the center o and the boundary $\partial\mathcal{B}^2$ the magnetic field is zero, therefore the geodesic rays ρ are orthogonal to $\partial\mathcal{B}^2$ with respect to the Randers metric F as well. Taking into account that the Riemannian length of the inward geodesic rays ρ from $\partial\mathcal{B}^2$ with respect to the Riemannian metric a is the same, then it can be seen that all inward geodesic rays emanating orthogonal to the boundary $\partial\mathcal{B}^2$ gather in the origin O and they have the same Finslerian length. $\square$

This construction can be easily extended to the case of an n-dimensional ball $\mathcal{B}^n \in \mathbb{R}^n$ with the Euclidean metric a. In this case, we can construct by the same procedure as above a Randers metric $(\mathcal{B}^n, F = \alpha + \beta)$, whose inward geodesics coincide to the geodesic rays from the boundary $\partial\mathcal{B}^n = \mathbb{S}^{n-1} \subset \mathbb{R}^n$ and whose inward cut locus is the center of the sphere $\mathbb{S}^{n-1}$.

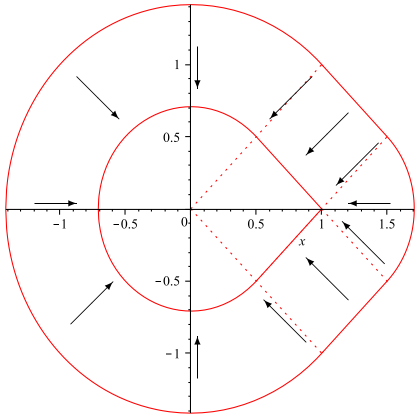

Fig. 9. The magnetic field defined within the convex ball H_0.

6. Proof of Theorem 1.2

As explained already the inward cut locus from the C^1-boundary ∂D_0 with respect to the usual Euclidean metric in $\mathbb{R}^2$ coincides with the segment oq. We are going to construct a Randers metric on the 2-ball D_0 whose inward cut locus of the boundary ∂D_0 is the same segment oq (see Fig. 9).

In order to write our formulas explicitly in polar coordinates (r, θ), for the sake of clarity and simplicity, we will consider the circles S and S' to be centered at the origin with radius $\sqrt{2}$, and at the point $A(1, 0)$ with radius $\frac{\sqrt{2}}{2}$, respectively. We also take $\phi = \frac{\pi}{4}$.

Remark that the 2-ball D_0 is made of three regions (compare with Fig. 2 and notations in Section 2):

(1) $(x, y) = (r_1 \cos\theta, r_1 \sin\theta) \in B(o, \sqrt{2})$, where $r_1 \in [0, \sqrt{2}]$, $\theta \in [\frac{\pi}{4}, \frac{7\pi}{4}]$, i.e. the large circular sector whose boundary is P;

(2) $(x, y) = (u + \dfrac{\sqrt{2}}{2}\rho + \dfrac{1-u}{2}, \pm\dfrac{\sqrt{2}}{2}\rho \pm \dfrac{1-u}{2})$, where $\rho \in [0, \dfrac{\sqrt{2}}{2}]$, $u \in [0, 1]$, i.e. a part of the central region whose boundary is A;

(3) $(x, y) = (r_2 \cos\theta, r_2 \sin\theta) \in B((1, 0), \frac{\sqrt{2}}{2})$, where $r_2 \in [0, \frac{\sqrt{2}}{2}]$, $\theta \in [-\frac{\pi}{4}, \frac{\pi}{4}]$, i.e. the small circular sector whose boundary is P_0.

We point out that (r_1, θ) and (r_2, θ) are polar coordinates in the balls $B(o, \sqrt{2})$ and $B((1, 0), \frac{\sqrt{2}}{2})$, while (ρ, u) are coordinates on the interior of the squares defined by the points $(\dfrac{1}{2}, \dfrac{1}{2})$, $(1, 1)$, $(\dfrac{3}{2}, \dfrac{1}{2})$, $(1, 0)$ and $(\dfrac{1}{2}, -\dfrac{1}{2})$, $(1, -1)$, $(\dfrac{3}{2}, -\dfrac{1}{2})$, $(1, 0)$, respectively. Nevertheless, we have $r_1 = \rho + \frac{\sqrt{2}}{2}$.

We are going to define a magnetic field β acting on the (inner) straight rays from the boundaries of each regions as follows.

$$\beta = \begin{cases} \beta_1 := -h_1(r_1)dr_1, & x \in \text{ region (1)} \\ \beta_2 := -h_2(\rho)d\rho, & x \in \text{ region (2)} \\ \beta_3 := -h_3(r_2)dr_2, & x \in \text{ region (3)} \end{cases} \tag{6.1}$$

defined on D_0, where $h_1 : [\frac{\sqrt{2}}{2}, \sqrt{2}] \to [0, 1)$, $h_2 : [0, \frac{\sqrt{2}}{2}] \to [0, 1)$ and $h_3 : [0, \frac{\sqrt{2}}{2}] \to [0, 1)$ are constructed as shown in Lemma 5.4 and Remark 5.5 (see Fig. 9).

By naturally extending β to the ball $\widetilde{D}_0$ with smooth boundary, then it can be easily seen that the Randers metric $(\widetilde{D}_0, F_0 = \alpha + \beta_0)$ is projectively flat and the cut locus of the hypersurface $\partial\widetilde{D}_0$ with respect to this Finsler metric is the segment oq. This can be easily done by extending the definition domain of

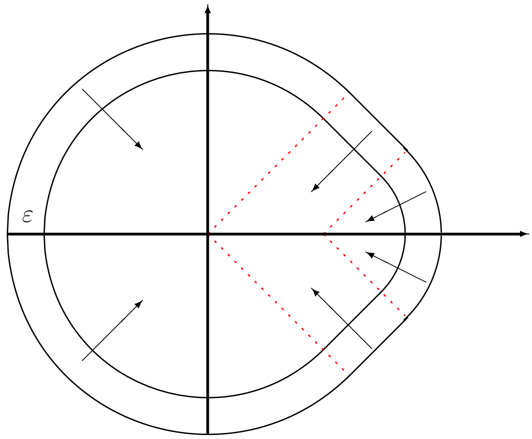

Fig. 10. The magnetic field extended in $\widetilde{D}_0$.

the functions h_i such that $h_{|\partial\widetilde{D}_0} = 0$, namely $h_1 : [\frac{\sqrt{2}}{2}, \sqrt{2}+\varepsilon] \to [0,1)$, $h_2 : [0, \frac{\sqrt{2}}{2}+\varepsilon] \to [0,1)$ and $h_3 : [0, \frac{\sqrt{2}}{2}+\varepsilon] \to [0,1)$, respectively (see Fig. 10).

This construction can be extended to arbitrary dimension and repeated iteratively for each depth level m such that we obtain

Proposition 6.1. *For each depth level m, there is a Randers metric $(\widetilde{D}_m, F_m = \alpha + \beta_m)$ on the smooth ball $\widetilde{D}_m \subset \mathbb{R}^n$ with the following properties*

1. *F_m is projectively flat,*
2. *the inner cut locus of the boundary $\partial\widetilde{D}_m$ with respect to F_m is the tree $s \cup s_{j_1} \cup \cdots \cup s_{j_1 j_2 \ldots j_m}$.*

This result is interesting in itself because it gives a simple example of Randers metric whose cut locus of a closed hypersurface is a tree (compare [14]).

At limit we obtain

Proposition 6.2. *There is a Randers metric $(\widetilde{D}, F = \alpha + \beta)$ on the smooth ball $\widetilde{D} = \lim_{m\to\infty} \widetilde{D}_m \subset \mathbb{R}^n$ with the following properties*

1. *F is projectively flat,*
2. *the inner cut locus of the boundary $\partial\widetilde{D}$ with respect to F is the infinite tree IT,*

where $F = \lim_{m\to\infty} F_m$.

We remark that, for any finite m, the magnetic field β_m defined here is initially defined inside regions (1), (2), (3) and extended by ε-dilatation. However, one can easily see that the regions (2) and (3), considered inside H_m, become smaller as m increases. At limit $m \to \infty$, the regions (2), (3) shrink to domains of Hausdorff dimension one and zero, respectively, in other words the intensity of magnetic field β inside H_m decreases to zero as m approaches infinity. Nevertheless, β is unchanged in region (1) and in the ε-dilatation of (2) and (3).

Proof of Theorem 1.2. Let us consider again the construction of the n-sphere $M = \mathbb{S}^n$ endowed with a Riemannian metric g such that g restricted to $M \setminus$ (interior of Δ) coincides with the initial metric a_{ij} defined on $\widetilde{D}$ (see the Proof of Theorem 1.1 in Section 4).

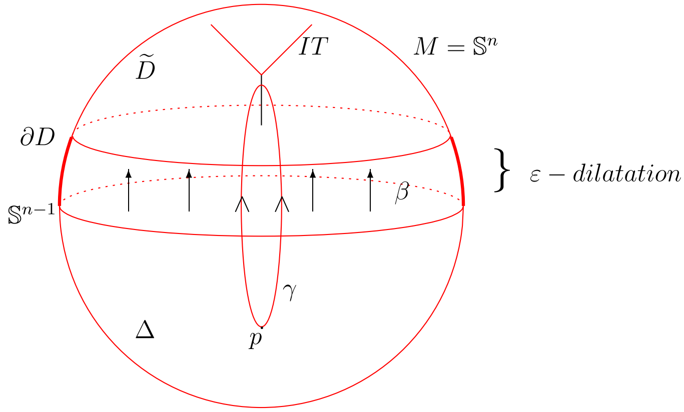

Fig. 11. The Randers metric on M with tropical magnetic field.

On the other hand, we have the magnetic field β defined above on $\widetilde{D}$. For the sake of simplicity we assume here that β actually acts only on the ε-dilatation region bounded by $\widetilde{H}$ and $\partial\widetilde{D}$.

From the discussion above it follows that the Randers metric $(M, g+\beta)$ is a Finsler metric on the n-sphere $M = \mathbb{S}^n$ whose cut locus is IT having the same order of differentiability with (M, g).

This magnetic field is acting only on the tropical region of the North Hemisphere.

Of course β is a closed 1-form and therefore the geodesics of the Randers metric $F = g + \beta$ coincide with the Riemannian geodesics of (M, g) as point sets (see Fig. 11).

The cut locus of p with respect to the Randers metric $F = g + \beta$ coincides with the infinite tree IT and since (M, g) is C^k, but not C^∞ this property is inherited by F as well and hence Theorem 1.2 is proved. $\square$

Remark 6.3. Actually, this magnetic field β can be extended in the interior of Δ. In this way we obtain a Randers metric whose magnetic field acts in all Δ.

Let us denote by $\gamma : [0, a] \to M$, $\gamma(0) = p$, $\gamma(a) = q$ a minimizing geodesic segment of (M, g) that joins the point p with a point $q \in \mathcal{C}(p)$. Using for example Riemannian geodesic coordinates, any geodesic segment from p to its cut point is a straight line. Then using Lemma 5.4 and Remark 5.5 we can extend the tropical magnetic field defined on the ε-dilatation region to entire hemisphere Δ.

Obviously, our magnetic field is zero at p, increases in strength and decreases again to zero after crossing the equator when moving from south to north such that β vanishes on ∂D.

References

[1] D. Bao, S.S. Chern, Z. Shen, An Introduction to Riemann Finsler Geometry, Graduate Texts in Mathematics, vol. 200, Springer, 2000.
[2] M. Buchner, Simplicial structure of the real analytic cut locus, Proc. Am. Math. Soc. 64 (1977) 118–121.
[3] M. Buchner, The structure of the cut locus in dimension less than or equal to six, Compos. Math. 37 (1978) 103–119.
[4] K. Falconer, Fractal Geometry, second edition, John Wiley & Sons, 2003.
[5] H. Gluck, D. Singer, Scattering of geodesic fields I, Ann. Math. 108 (1978) 347–372.
[6] J. Itoh, The length of a cut locus on a surface and Ambrose's problem, J. Differ. Geom. 43 (1996) 642–651.
[7] J. Itoh, K. Kiyohara, The cut loci and the conjugate loci on ellipsoids, Manuscr. Math. 114 (2004) 247–264.
[8] J. Itoh, M. Tanaka, The dimension of a cut locus on a smooth Riemannian manifold, Tohoku Math. J. 50 (1998) 571–575.
[9] Y.Y. Li, L. Nirenberg, The distance function to the boundary, Finsler geometry, and the singular set of viscosity solutions of some Hamilton–Jacobi equations, Commun. Pure Appl. Math. 58 (1) (2005) 85–146.
[10] S.B. Myers, Connections between differential geometry and topology I, Duke Math. J. 1 (1935) 376–391.
[11] S.V. Sabau, H. Shimada, Finsler manifolds with reversible geodesics, Rev. Roum. Math. Pures Appl. 57 (1) (2012) 91–103.
[12] Z. Shen, Lectures on Finsler Geometry, World Scientific, 2001.
[13] K. Shiohama, M. Tanaka, Cut loci and distance spheres on Alexandrov surfaces, in: Actes de la Table Ronde de Géométrie Différentielle en l'honneur Marcel Berger, in: Séminaries & Congrès, Collection SMF No. 1, 1996, pp. 531–560.
[14] M. Tanaka, S.V. Sabau, The cut locus and distance function from a closed subset of a Finsler manifold, preprint.
[15] A. Weinstein, The cut locus and conjugate locus of a Riemannian manifold, Ann. Math. 87 (1968) 29–41.